Applied Acoustics 219 (2024) 109920

Contents lists available at ScienceDirect

Applied Acoustics

journal homepage: www.elsevier.com/locate/apacoust

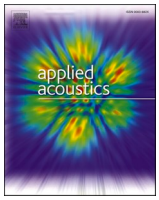

Sound transmission across a rectangular duct section with a thin micro-perforated wall backed by a sidebranch cavity

M.L. Fung [a], S.K. Tang [b,*], Mors Leung [c]

[a] Department of Building Environment and Energy Engineering, The Hong Kong Polytechnic University, Hong Kong, China
[b] School of Engineering, The University of Hull, Hull HU6 7RX, United Kingdom
[c] Architectural Acoustics (International) Limited, Hong Kong Special Administrative Region

ARTICLE INFO

Keywords:
Sound transmission
Micro-perforation
Duct noise control

ABSTRACT

An experimental investigation was carried out in the present study for deeper understanding on the sound transmission across a rectangular duct section installed with a thin micro-perforated panel (as a duct wall) backed by a sidebranch cavity. The contributions of the panel configuration and the cavity depth on reducing sound transmission are examined in detail. Results indicate a complicated relationship between sound power transmission, micro-perforation configuration and backing cavity depth. For panels with strong sound absorption capacity, sound power transmission efficiency is reduced as the panels become less absorptive, but there exists a frequency or frequency band above which the opposite is observed. It appears that there is also a certain level of panel sound absorption below which the sound transmission is strengthened over the whole frequency range of present study when the panel becomes less absorptive to sound.

1. Introduction

Controlling noise from the fans of the air conditioning and ventilation systems in modern heavily serviced commercial buildings effectively has long been a challenging topic for engineers and acousticians. These noises propagate into the occupied zones of the buildings and can have many adverse effects on the occupants if they are not attenuated properly [1]. Though noise control criteria have been established for years (for instance, Beranek [2]), flow duct silencing devices are the key elements in the noise control process.

Conventional noise mitigation method is to use dissipative silencers, which are flow restrictions lined with porous materials (e.g. rockwool) [3]. These devices offer good sound reduction at frequencies higher than 500 Hz in general, but their low frequency performance is not satisfactory because of the lattice structures of the porous materials [3]. Also, the porous materials are not suitable for use in the building air ductwork as the dirt/grease/moisture there will eventually clog the tiny pores of these materials, rendering them useless for noise control if the silencers are not properly maintained. In addition, the porous materials will disintegrate during use. The very fine material fibres will then go into the occupied zones together with the treated air, increasing the indoor air particulate level and affecting adversely the health of the occupants. The relatively high static pressure losses across these devices [3] result in significant energy wastage and is a big concern nowadays under the concepts of sustainability as well as carbon-neutrality.

Reactive silencing devices, such as the Helmholtz resonators [4], have been proposed in the past few decades. Though these resonance-based devices will result in only limited static pressure loss, they in general cannot offer broadband noise reduction unless they are carefully coupled together. Typical examples include the sidebranch array mufflers [5], the coupled resonators [6–8] and the meta-material-based silencers [9], but this list is by no mean exhaustive. The structures of these devices, however, are usually relatively complicated and they are bulky in general, making them not easy to fit into the congested ceiling voids in modern commercial buildings. Stringent selection of resonance frequencies of the coupling components is also required.

Maa [10] introduced the theory of micro-perforated panel absorbers (MPPA), and since then MPPA have attracted much attentions (for instance, Liu et al. [11], Sakagami et al. [12] and Bravo et al. [13]). Backed by a rigid cavity, MPPA can offer good sound absorption at frequencies much lower than those of the dissipative silencers [11,14]. Allam and Åbom [15] investigated its use in circular duct silencers, Takahashi and Tanaka [16] studied the effect of panel vibration on the sound absorption characteristics of the MPPA under normal sound

* Corresponding author.
E-mail address: S.Tang@hull.ac.uk (S.K. Tang).

https://doi.org/10.1016/j.apacoust.2024.109920
Received 16 November 2023; Received in revised form 19 January 2024; Accepted 14 February 2024
Available online 22 February 2024

incidence, Wang et al. [17] examined the effect of irregular MPPA cavity, and this list is again by no mean exhaustive. In principle, a MPPA silencer offers very low flow resistance and a low risk of health hazard, and can easily be maintained, making this type of silencers an important alternative to the dissipative silencers and the coupled reactive devices. Despite its importance, a parametric analysis on the sound transmission and absorption across a MPPA duct silencer is rarely found in existing literature, at least to the knowledge of the authors.

A detailed experimental investigation is carried out in the present study in order to understand how the micro-perforated panel (a duct wall) configurations and the backing cavity depth affect the sound propagation across a MPPA silencer in a rectangular duct. Attention will also be paid on the effects of cavity acoustic modes and panel vibration modes on the spectral sound transmission characteristics. The results will contribute directly to the development of a low-static-pressure-loss broadband compact duct silencer.

2. Experimental setup

Fig. 1 illustrates the schematics of the test rig and the nomenclatures adopted in the present study. The test rig, except the test section, was similar to those previously used by the corresponding author (for instance, Yu and Tang [18] and Tang and Tang [19]). It consisted mainly of a quiet flow facility, a 6-inch aperture wall-mounted loudspeaker, a test section and an anechoic termination designed based on the recommendations of Neise et al. [20]. It has been shown previously that the sound power reflection coefficient of this termination is less than 0.04 at frequencies higher than 200 Hz. The duct height and the duct span were 173 mm and 150 mm respectively, giving the first higher mode cut-on frequency at around 991 Hz. The walls of the duct (except that of the perforated panel) and the test section were made of 20 mm thick acrylic to avoid unnecessary vibration and sound breakout problem.

The length of the MPPA silencer tested was fixed at 720 mm, while the backing cavity depth, D, was varied from 40 mm to 160 mm in intervals of 40 mm. The acrylic micro-perforated panels (MPP), clamped on its four sides between the cavity and the main duct, were of thicknesses (t_p) of 1.8 mm and 2.6 mm. The micro-perforations on the panels were produced by laser punching and were elliptic in shape and tapered because of the characteristics of the laser punching process [14]. Spacing between perforations (s_p) was 2.5 mm and 4.0 mm. A total of 48 MPPA silencer models were tested (excluding those with non-perforated panels). Table 1 summarizes the details of the MPPs adopted in the present study. Fig. 2 shows two examples of these panels. During the measurement, white noise signal of constant magnitude was fed to the loudspeaker via a suitable power amplifier. Owing to the above-mentioned limitations of the flow assembly, the frequency range of the present study is from 200 Hz to 900 Hz.

Four Brüel & Kjær Type 4935 1/4 in. microphones were used to capture the acoustic signals on the two sides of the test section. They were located more than 2.5 times the duct widths away from the test section where the evanescent waves should be insignificant. The data recorder was a Brüel & Kjær Type 3506D PULSE system, and the sampling rate was 4096 samples per second per channel. The four-microphone method for plane wave analysis was adopted to estimate the sound power transmission coefficient, τ, and the complex sound pressure reflection coefficient, r, of the MPPA silencers from the acoustic signals recorded. This method has been explained thoroughly by Tang and Li [21] and Chung and Blaser [22], and thus it is not repeated here. The corresponding sound power absorption coefficient α can be obtained by observing that

$$\alpha = 1 - \tau - |r|^2. \tag{1}$$

One should note that α will increase with increasing cavity length to duct height ratio.

The fan of the present test rig could produce a flow speed of 12 m/s within the test section. However, it was found that the sound power transmission across the MPPA silencer models was not affected much by the flow, except that the sound transmission spectra became relatively more spurious at increased flow speed (not shown here). This tends to suggest that the effects of duct flow on the panel vibration and the sound absorption of the MPPs are not significant within the parameter boundary of the present study. The foregoing discussions are thus focussed on the 'no flow' cases.

3. Results and discussions

It is believed that the viscous energy dissipation at the perforations of the MPPs, and the vibration and structural damping of these panels are the major mechanisms leading to sound reduction across the silencer models (Fig. 3). As the sound reduction mechanisms of the cavity backed MPP and the related physics are much more complicated that those of the locally reacting Cremer-type impedance absorption [23,24], a

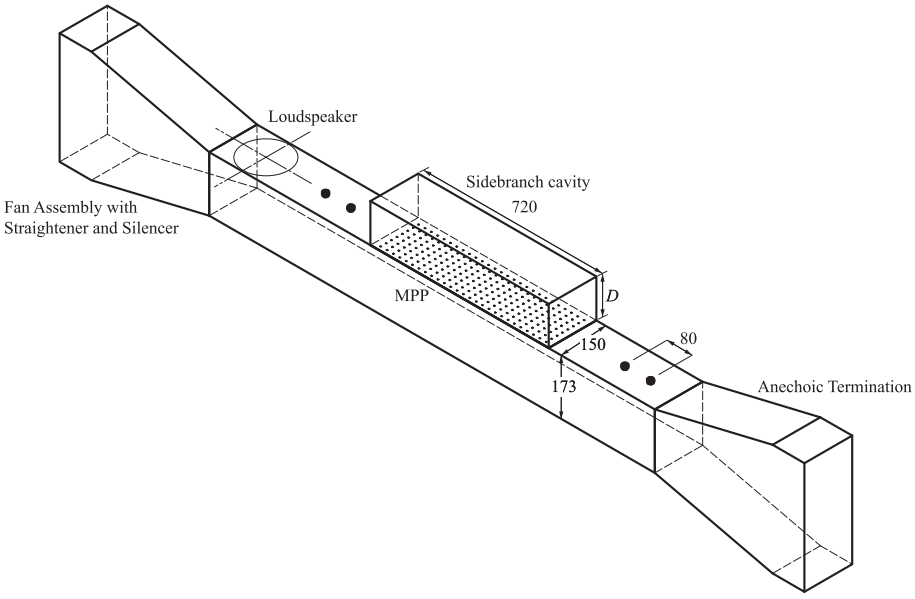

Fig. 1. Schematics of the test rig assembly. All dimensions in mm; ●: microphones.

Table 1
Configurations of the MPPs tested (all length scales in mm).*

Panel	t_p	w_d	h_d	e_d	w_c	h_c	e_c	s_p	$\alpha_{n,peak}$	Sound absorptivity
P01	1.8	0.34	0.24	0.71	0.22	0.16	0.69	2.5	0.34	Weak
P02								4.0	0.15	Weak
P03		0.38	0.32	0.54	0.36	0.26	0.69	2.5	0.83	High
P04								4.0	0.48	Moderate
P05		0.46	0.34	0.67	0.40	0.32	0.60	2.5	0.97	High
P06								4.0	0.69	Moderate
P07		Panel without perforations								
P08	2.6	0.44	0.28	0.77	0.18	0.12	0.75	2.5	0.27	Weak
P09								4.0	0.12	Weak
P10		0.44	0.30	0.73	0.38	0.24	0.78	2.5	0.72	Moderate
P11								4.0	0.39	Moderate
P12		0.52	0.36	0.72	0.50	0.34	0.73	2.5	0.98	High
P13								4.0	0.73	Moderate
P14		Panel without perforations								

* w and h: width and height of ellipse respectively, e: eccentricity. Suffix d: duct side, c: cavity side.

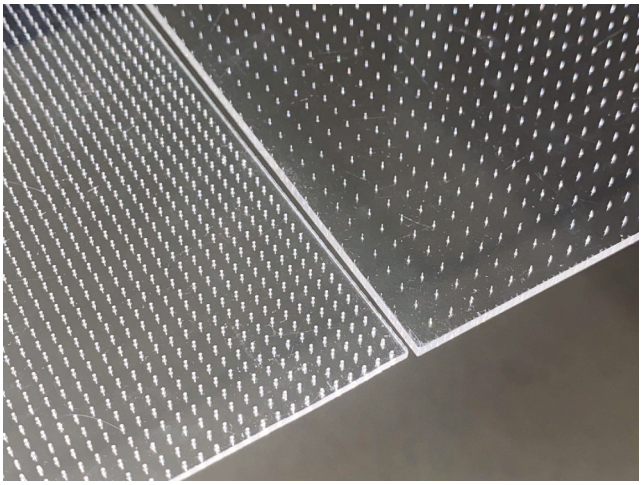

Fig. 2. Examples of the MPPs used in the experiment. Left: P05; right: P09.

comparison of the MPP impedances with the optimized Cremer impedance is not presented. Before analysing the sound transmission across the MPPA silencer models and the effects of the micro-perforations on the transmission, it is essential to have basic understanding on the sound absorption characteristics of the MPPs involved and the coupling between the cavity acoustics and the panel vibrations.

3.1. Sound absorption of MPPs under normal sound incidence

Fig. 4 shows the spectral variations of sound absorption, α_n, of the cavity-backed MPPs adopted in the present study upon normal sound incidence estimated using the elliptic perforation formula of Fung et al. [14]. It is noticed that the sound absorption capability of a cavity-backed MPP is stronger at higher perforation density provided that other parameters are kept fixed. Also, smaller perforation size leads to weaker sound absorption and a lower peak absorption frequency, while a larger D does not affect much the magnitude of the sound absorption but it shifts the absorption spectrum to the lower frequency side. The effect of panel thickness is not insignificant probably because of the small change in the thickness in the experiment. However, it appears that a thicker panel reduces the peak absorption frequency.

It should be noted that we have a grazing incidence condition in the experiment, and thus the effects of these panels will not be as strong as

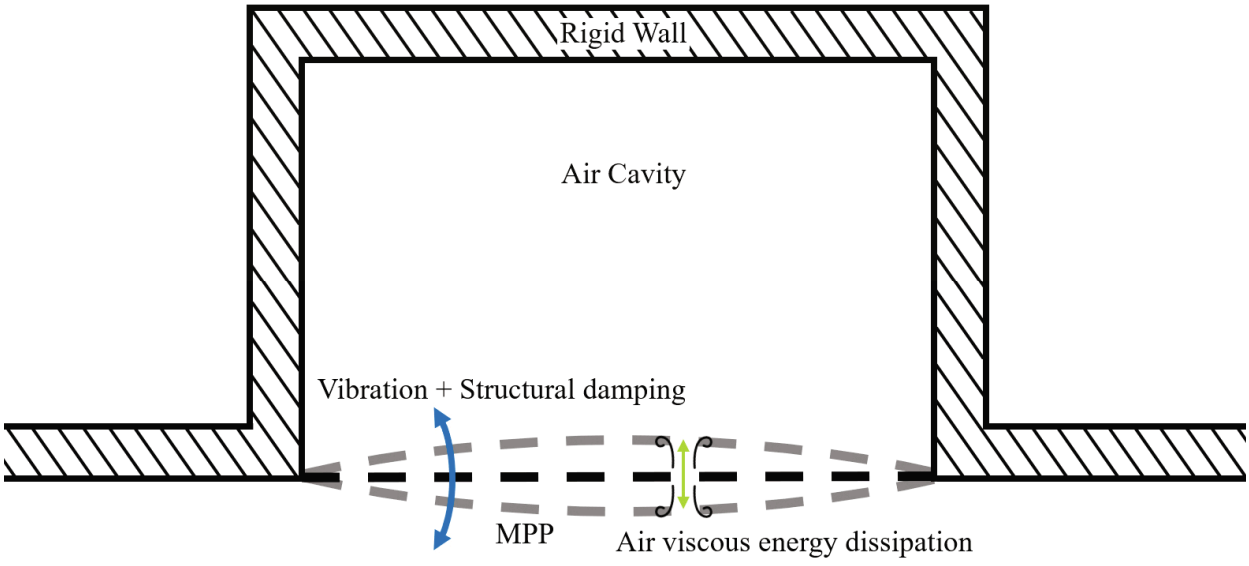

Fig. 3. Expected major sound reduction mechanisms of a MPPA silencer model.

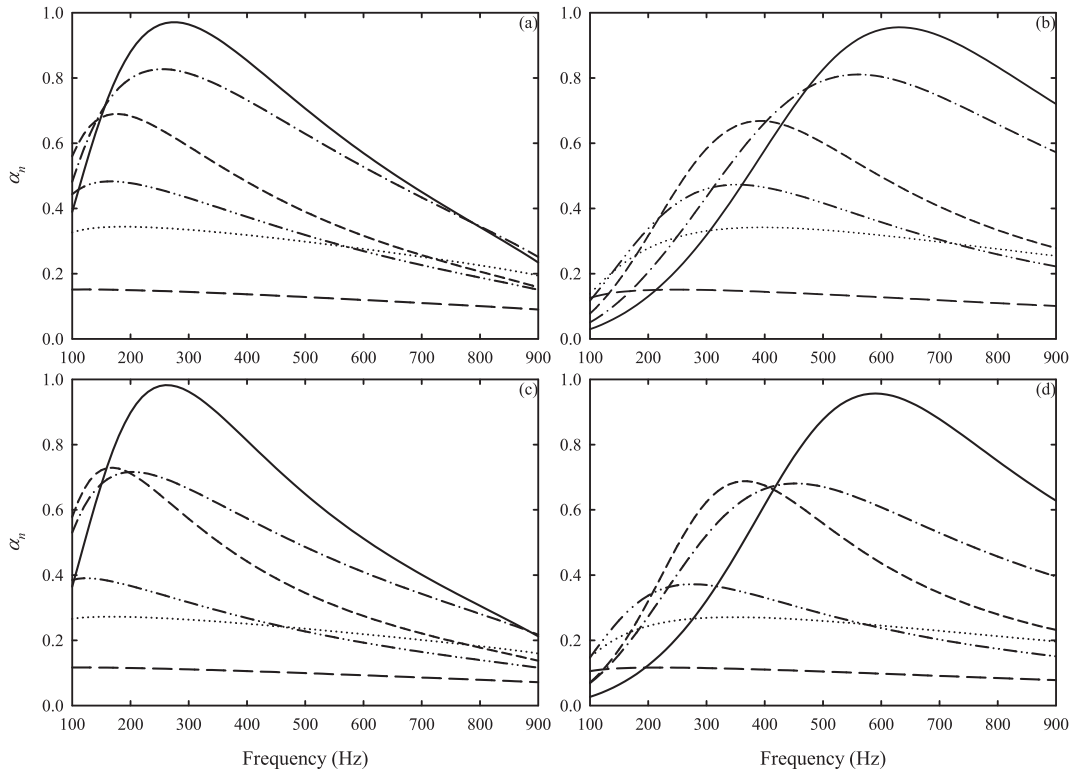

Fig. 4. Estimated normal incidence sound absorption coefficients of cavity-backed MPPs. (a) $t_p = 1.8$ mm, $D = 160$ mm; (b) $t_p = 1.8$ mm, $D = 40$ mm; (c) $t_p = 2.6$ mm, $D = 160$ mm; (d) $t_p = 2.6$ mm, $D = 40$ mm. · · · · · · · ·: P01/P08; — — —: P02/P09; — · —: P03/P10; — ·· —: P04/P11; ————: P05/P12; – – – – –: P06/P13;

those shown in Fig. 4. One can also observe that the sound absorptions of the cavity-backed MPPs P01/P02 and P08/P09, on which the perforations are the smallest and most tapered, are very weak.

3.2. Coupling of cavity acoustics and panel vibration

It is believed that the micro-perforations do not have strong influence on the macroscopic panel vibration modes as can be inferred from the work of Lee et al. [24] and Bravo et al. [25]. Panels P07 and P14, which are not perforated, are thus used here to illustrate the basic cavity-panel coupling. For the sake of easy reference, the vibration mode and the acoustic cavity mode eigen-frequencies are denoted hereinafter by $f_{p,m,n}$ and $f_{c,m}$ respectively, where the suffices m and n are integers denoting the mode order in the longitudinal and spanwise direction respectively. Within the frequency range of the present study, only the longitudinal planar cavity acoustic modes are important due to the relatively short cavity width (150 mm) and depth ($\leq$160 mm). These values of width and depth of the cavity give rise to acoustic modes in the width-wise and depth-wise of eigen-frequencies higher than 900 Hz. Also, as the upstream excitation is planar in the present experiment, those spanwise asymmetrical vibration modes are not significant (those with an odd n).

Fig. 5 shows the spectral variations of τ and α of P07 and P14 when they are backed by cavities of different depths. It is found that $\tau \approx 1$ and $\alpha \approx 0$ for their 'no cavity' counterparts (not shown here), and these data are not discussed in the foregoing analyses. Also, it should be noted that the sound power reflection of the anechoic termination is higher than 4 % at frequencies below 150 Hz. Therefore, the data at that frequency range could be less accurate. Nevertheless, it can be observed from Fig. 5a and b that the spectral variations of τ and α are highly correlated. A dip in τ corresponds to a local peak in α. The sound power reflection is basically negligible. In fact, this is in principle true for all the other MPPA silencer model cases in the present study. Thus, the complex sound pressure reflection coefficients, r, are not further discussed hereinafter. The peak sound absorption frequencies decrease as the cavity depth D increases. Fig. 5c and d shows that the increase in panel thickness also results in a shift of the peak absorption frequencies to the lower side of the sound absorption/transmission spectrum. In addition, one can notice that the effect of D becomes much less significant for $D \geq$ 120 mm. This will be further discussed later.

As these panels are not perforated, the reduction in sound power transmission across the MPPA silencer models are mainly due to structural damping, which are highly related to the vibration modes of the panels under the influence of the acoustic modes within the backing cavity [26] and the acoustic impedance of the main duct of the test section. One can observe from Fig. 5 that τ is usually close to unity (also $\alpha \to 0$) at the eigen-frequencies of the cavity acoustic modes, except near to the first longitudinal higher mode cut-off cavity frequency, $f_{c,1}$, where the panel vibration modes are better excited.

The corresponding *in-vacuo* panel vibration mode eigen-frequencies are estimated using the formula given in Leissa [27] and indicated in Fig. 5. The spanwise odd vibration mode eigen-frequencies are not presented as the present plane wave excitation does not favour the excitation of these modes. One can observe from Fig. 5a that the τ dip frequencies within the proximity of $f_{c,1}$ appear to converge to $f_{p,3,2}$ and $f_{p,9,2}$ as D increases. The reduction of the cavity stiffness relative to that of the panel at increased D tends to decouple the cavity and the panel such that the panel eventually is more free to vibrate at its own eigen-frequencies [26]. For shallower cavity (shorter D), the stronger coupling between the cavity and the panel gives rise to the co-existence of various vibration modes as shown also in Pretlove [26]. Longitudinal symmetrical modes, such as those with eigen-frequencies $f_{p,4,2}$, $f_{p,6,2}$, $f_{p,8,2}$ and $f_{p,10,2}$ are likely to be excited at the same time.

One should note that the test model setup also resembles an expansion chamber, especially when the cavity stiffness is weak, such that there could be relatively lower sound power transmission across the test section at a frequency around $f_{c,1}/2$ [28]. In addition, at frequencies below $f_{c,1}$, the air inside the cavity could act like an elastic mass as that in the cavity of a Helmholtz resonator, resulting in low frequency

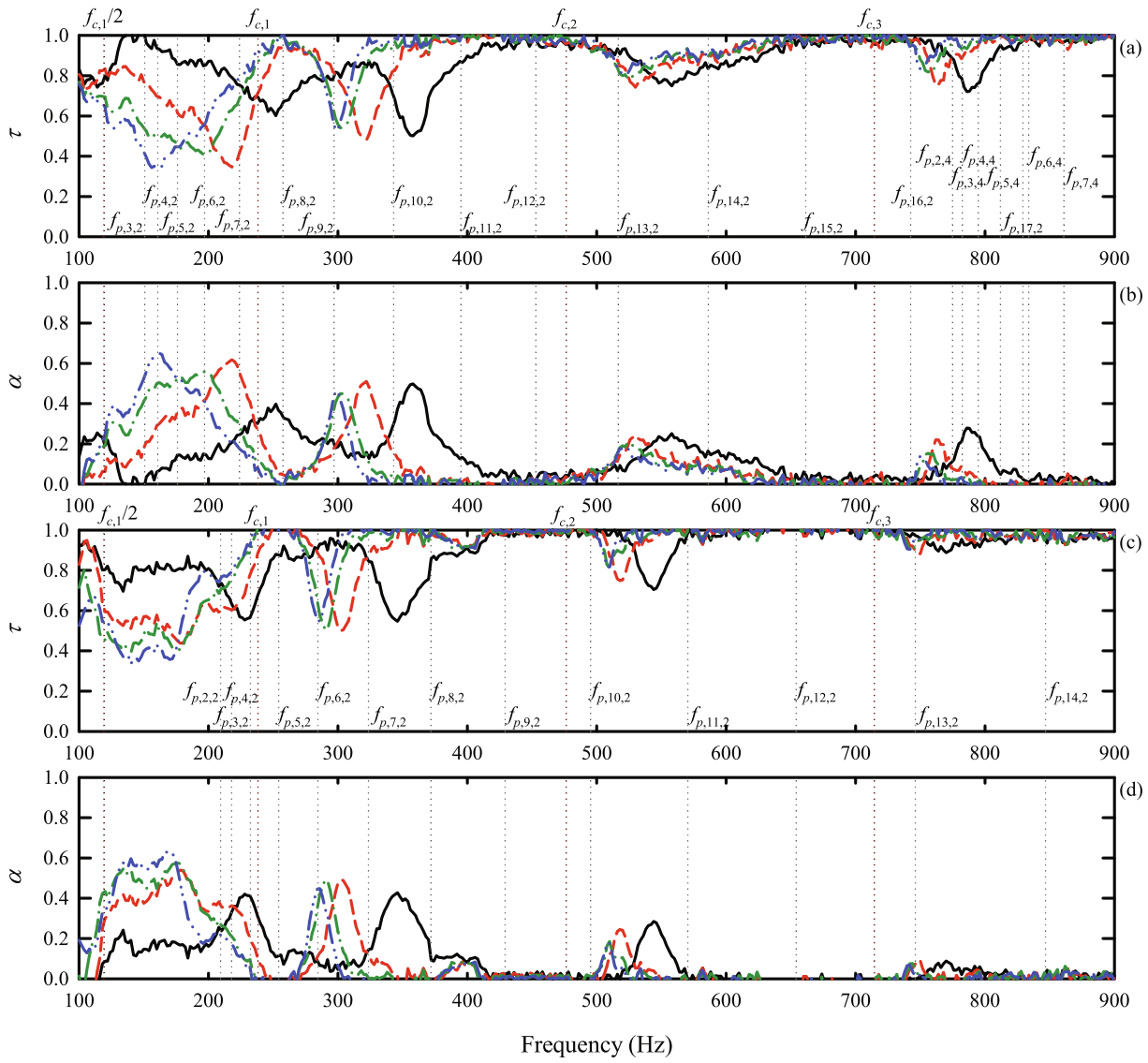

Fig. 5. Spectral variations of τ and α of test models with P07 and P14. (a) τ, P07; (b) α, P07; (c) τ, P14; (d) α, P14. ———: $D = 40$ mm; – – – – –: $D = 80$ mm; — · —: $D = 120$ mm; — ·· —: $D = 160$ mm.

resonance and relatively lower τ. However, owing to the limitation of the test rig, the results below 200 Hz will not be further discussed.

At frequencies around $f_{c,2}$, the sound field inside the cavity is likely to be lengthwise symmetrical with nodal planes at a quarter and 3 quarters of the cavity length. However, the panel vibration mode excited is the odd (13,2) mode and might be also the even (14,2) mode. The latter appears more important as the cavity stiffness increases (D decreases). The opposite is observed at around $f_{c,3}$ where the even panel vibration mode (16,2) is excited. This frequency is also close to $f_{p,2,4}$, $f_{p,3,4}$, $f_{p,4,4}$ and $f_{p,5,4}$, but it is not believed that the corresponding vibration modes are effectively excited as these $n = 4$ vibration modes result in relatively higher bending stresses along the span of the panel and thus the damping should be strong. However, they can briefly exist under the strong cavity-panel coupling as D decreases.

The transmission around $f_{c,2}$, $f_{c,3}$, $f_{p,12,2}$ and $f_{p,15,2}$ is relatively strong. As the sound power reflection coefficient is small over the whole frequency range of the present study, the panel vibration must be so weak that structural damping becomes insignificant such that $\alpha \to 0$ and $\tau \to 1$. This will be discussed further later.

The increase of panel thickness t_p results in the excitation of different vibration modes as shown in Fig. 5c. At $t_p = 2.6$ mm, $f_{p,m,4}$s are all higher than 1000 Hz. The major vibration modes excited are the (2,2), (6,2), (10,2) and (13,2) modes, while more modes could have been excited as D is reduced as explained before. One can notice from Fig. 5a and c that at frequencies higher than $f_{c,2}$, the panel vibration mode excited is of an eigen-frequency just above that of the cavity acoustic mode. Just above $f_{c,1}$, it is the second next higher vibration mode which is excited instead.

Overall, one can observe that P07 and P14 do not offer significant resistance to sound transmission, especially at frequencies higher than 400 Hz. The broadband sound absorption of the MPPs as shown in Fig. 4 should be very helpful in improving the bandwidth of the sound reduction.

3.3. Effects of perforations on sound transmission

3.3.1. Sound transmission and acoustic impedance of MPPA silencer model

Fig. 6a shows the spectral variations of τ of the MPPA silencer models installed with panel P05 ($t_p = 1.8$ mm) at different cavity depths D. This panel is supposed to give the highest normal incidence sound absorption coefficient among all panels tested in the present study. It should be noted that the spectral variations of the corresponding α are just basically opposite those of τ as $|r|$ is very small.

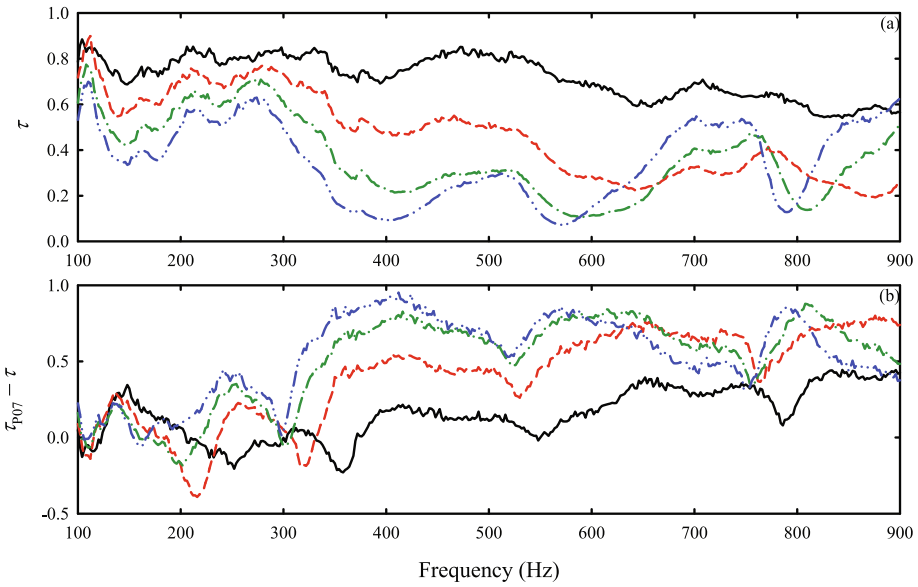

Fig. 6. Sound power transmission coefficients of MPPA silencer installed with P05. (a) τ; (b) Improvement over P07. Legends: same as those of Fig. 5.

It is observed that τ increases with increasing D in general for frequencies below ~600 Hz. Within this frequency range, one can notice that the kind of relatively sharp τ dips at or near to the vibration mode eigen-frequencies (c.f. Fig. 5a) are not explicitly found. The viscous energy dissipation of the perforations appears to have provided some damping to the panel vibration. It is also observed that a stronger sound absorption capacity of the MPP tends to weaken τ. This tends to suggest that within this frequency range, the sound absorption effect of the MPP is less important than the energy dissipation by structural damping. The higher reduction in the panel vibration overrides the benefit of MPP sound absorption, resulting in an increase in transmitted sound power. Besides, the acoustic impedance of the MPP is modified by the panel vibration, and the peak absorption frequency could increase for thin panel [16].

At frequencies higher than 600 Hz, τ first decreases with increasing D. It reaches a minimum and then increases as D is further increased, except at frequencies around 800 Hz, where some panel vibration mode eigen-frequencies are located. The latter phenomenon is only found at relatively large D where the coupling between the cavity and the panel is expected to be weaker because of reduced cavity stiffness. It should be noted that the sound absorption of the MPP at larger D is less significant in this frequency range as well (see Fig. 4a). It appears that for $D \geq 120$ mm, the panel vibration, and thus the structural damping, has a strong influence on the acoustical performance of the MPPA silencer model in this frequency range. The structural damping due to viscous energy dissipation by the MPP has become less significant.

Fig. 6b illustrates the reduction of sound power transmission with P07 replaced by the perforated P05. At $D = 40$ mm, P05 does not provide much improvement, but a stronger sound transmission due to attenuation of panel vibration at lower frequencies. As D increases, the low frequency sound absorption becomes stronger and some improvement of τ can be found between 200 Hz and 300 Hz, where $\tau \approx 1$ without the perforations. The sound absorption produced by the MPPs does help reduce sound transmission, but again a stronger sound absorption capacity does not necessarily imply lower sound power transmission, especially when structural damping has more significant contribution to the overall sound transmission.

In simple term, the cavity-backed MPP duct wall behaves somewhat like the narrow sidebranch array mufflers of Yu and Tang [18] and the acoustic black holes (for instance, Zhang and Li [29] and Bravo and Maury [30]). It creates an impedance change within the main duct, causing upstream reflection, and attenuates sound further during its passage across the MPPA silencer model due to structural damping and sound absorption of the MPP. Though the impedance change may not fully reflect the sound absorption within the silencer, it should provide important information regarding the sound reduction because of the cavity-panel coupling. For simplicity, we express the acoustic impedance at the leading edge/entrance of the silencer model, Z, as

$$Z = (1 + \Delta Z) Z_{duct}, \tag{2}$$

where Z_{duct} is the acoustic impedance of the main duct section and ΔZ the impedance change normalized by Z_{duct}. The case of $|\Delta Z| = 0$ implies no sound reflection at the entrance of the silencer model but it does not necessarily suggest high sound transmission. In fact, this condition will lead to stronger sound energy propagation into the silencer and dissipation by the MPP actions, resulting in considerable sound reduction across the MPPA silencer. The impedance Z can be obtained by observing the phase differences of the incident and reflected waves due to the distance between the leading edge of the silencer model and the most upstream microphone, d (=540 mm in the present study):

$$Z = \frac{e^{-2jkd} + r}{e^{-2jkd} - r} Z_{duct} \Rightarrow \Delta Z = \frac{2r}{e^{-2jkd} - r}, \tag{3}$$

where k is the wavenumber of the sound and $j = \sqrt{-1}$.

ΔZ at $D = 40$ mm and 160 mm when P05 is installed are shown in Fig. 6a and b respectively. The corresponding τs are presented for the sake of easy reference. At $D = 40$ mm, the magnitude of ΔZ is small under the high cavity stiffness and the expected stronger cavity-panel coupling, suggesting that sound power reflection is overall weak. The resistive and reactive parts of ΔZ fluctuate about 0, and a rapid spectral variation of ΔZ is noticed. In fact, that of P07 are even more rapid while the corresponding ΔZ magnitude is weaker (not shown here). It should be noticed that there are many occasions where the resistance in ΔZ vanishes, while its reactance is at a local peak or dip. One distinctive example can be found at ~370 Hz, where a τ dip is observed and a relatively prominent τ dip of P07 is also found (Fig. 5a). The relatively strong reactance there in Fig. 6a suggests ΔZ is due to a mass-spring (panel-cavity) system, and thus a resonant panel vibration. Similar phenomenon can again be noted at ~150 Hz, ~250 Hz, between 500 Hz and 600 Hz, ~670 Hz, ~770 Hz and ~840 Hz, but the former could be a bit less accurate because of the limitation of the test rig. These are all near to the τ dips of P07 and/or an *in-vacuo* panel vibration eigen-frequencies of P07. The sound absorption of P05 results in broadband

sound attenuation and thus masks some of the τ dips of P07. This further echoes to the results of Lee et al. [24] and Bravo et al. [25] that the introduction of the micro-perforations does not basically alter much the vibration characteristics of the panel. There are also cases where ΔZ is purely resistive. The small derivation of ΔZ from unity implies some sound reflections upstream, which is not so positive to sound reduction as the efficiency of the MPP sound attenuation is then reduced.

The spectral variation of ΔZ resembles that of the duct with a side-branch [28] when D is increased to 160 mm, especially at frequencies higher than 400 Hz. Under a weaker cavity-panel coupling, the small and rapid fluctuations of ΔZ magnitude of the corresponding P07 cases (not shown here) are smoothed out and replaced by the much less rapid but larger ΔZ variations as shown in Fig. 7b. Again, lower τ and/or a decreasing τ can be observed near to the frequencies where a purely reactive ΔZ is found. However, exceptions are seen at ~490 Hz and ~710 Hz. These frequencies are close to $f_{c,2}$ and $f_{c,3}$ respectively. If one considers the test section as an expansion chamber, these frequencies are associated with strong sound transmission [31] because the standing wave within the chamber gives rise to strong sound pressure fluctuations at its two ends. The higher τ around 240 Hz (~$f_{c,1}$) is believed to be due to same reason. One can also notice similar phenomenon in Fig. 7a. It is believed that the negligible sound reduction of P07 around these frequencies (Fig. 5a and c) is also resulted from such standing wave excitation.

One can observe from Fig. 7b that there are occasions where ΔZ is purely resistive with a resistance considerably lower than 1. They are found near to relatively broadband τ dips (at around 435 Hz, 584 Hz and 762 Hz). Again, with the expansion chamber analogy, this kind of ΔZ characteristics, which occurs when the chamber length is equal to an odd integer multiple of a quarter wavelength of a sound, does not favour sound transmission [31]. It is interesting to note that these frequencies fall approximately into a geometrical progression with a multiplication factor of 4/3, but they do not match with the current test section length of 720 mm. It is conjectured that the panel vibration could have affected the effective length of the test section as seen by a sound wave. This is left to further investigations.

One can further observe from Fig. 7 that the low frequency ΔZ characteristics (below 400 Hz) are not much changed by D. One can find purely reactive ΔZ at similar frequencies, suggesting that the low frequency panel vibrations are relatively robust under the change in cavity stiffness.

3.3.2. *Effects of MPP configuration*

Fig. 8 illustrates the spectral variations of τ of MPPA silencer models installed with other 1.8 mm thick MPPs. One can again observe that the introduction of MPPs results in a general broadband reduction of sound transmission, though there are limited cases at low frequencies where the structural damping due to panel vibration could have been attenuated by the MPPs. The MPPs are in principle effective within the frequency range of the present study.

Fig. 8a shows the results of P06. The difference between P05 and P06 is the perforation separation s_p. P06 has a larger s_p and thus a significantly lower normal incidence sound absorption capacity in general. The peak sound absorption coefficient of P06 also appears at lower frequency, and it is consistent with the observed lower dip frequencies of P06 for all Ds for frequencies below 500 Hz. The τ of P06 MPPA silencer model is in general lower than that of its P05 counterpart at this frequency range, showing again a stronger sound absorption capacity of MPP is not an advantage at low frequencies. At higher frequencies, the sound absorption of P06 is significantly less than that of P05. The panel vibration gradually becomes more influential in shaping the sound transmission patterns at larger D, and thus the sharper τ dips at around

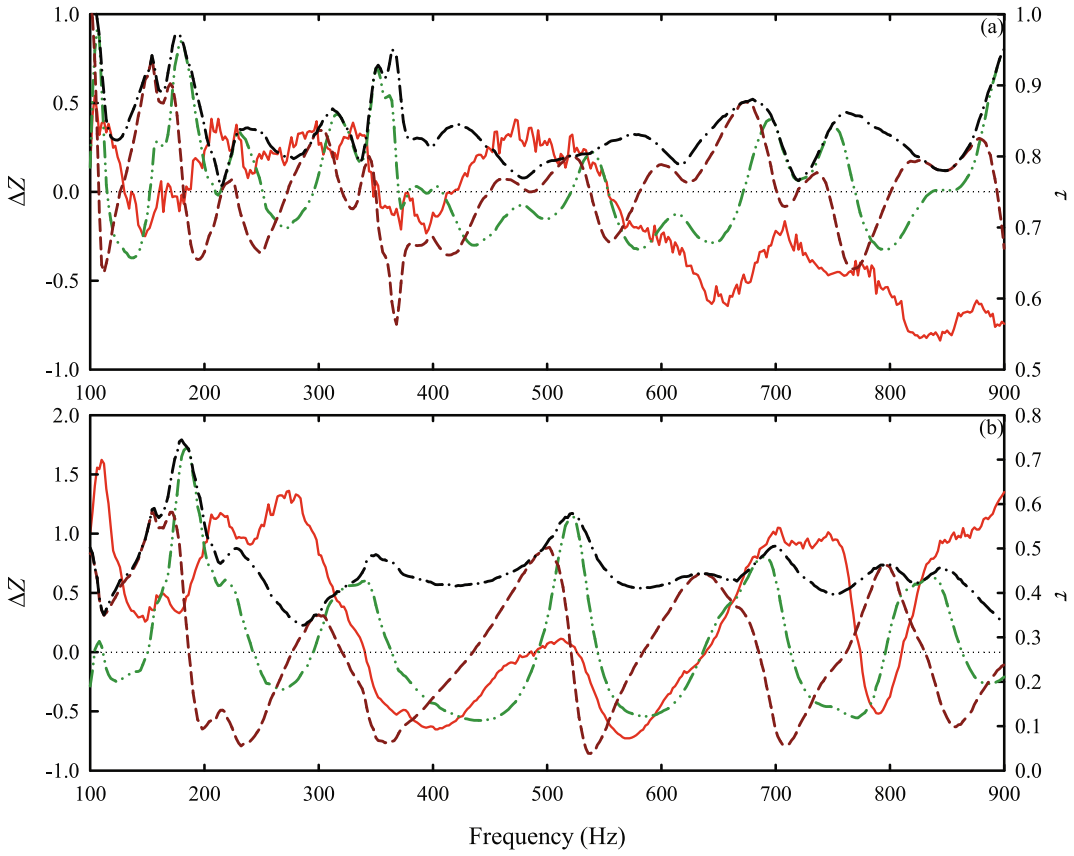

Fig. 7. Spectral variations of acoustic impedance change ΔZ of the test section with P05. (a) $D = 40$ mm; (b) $D = 160$ mm. ———: τ; — ·· —: Real(ΔZ); – – – – –: Imag(ΔZ); — · —: $|Z|$.

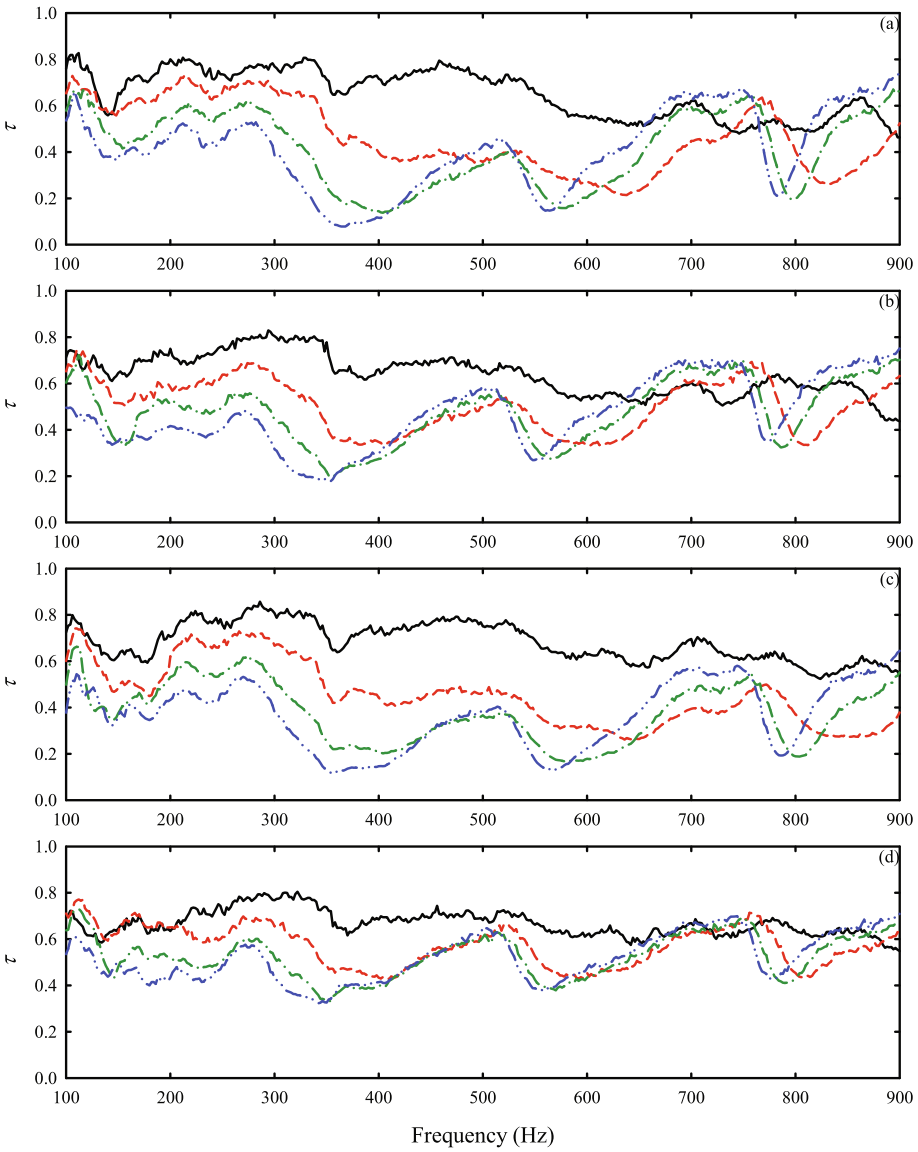

Fig. 8. Ffects of mpps on sound power transmission across the silencer model. t_p = 1.8 mm. (a) P06; (b) P04; (c) P03; (d) P01. Legends: same as those of Fig. 5.

800 Hz. Sound transmission at this frequency range is in general higher than that achieved with P05 when D is relatively large under the diminishing effects of the MPP. However, improvement below 700 Hz is still observed at $D = 40$ mm where the cavity-panel coupling is relatively stronger.

The sound absorption capacities of P04 and P03 are weaker than those of P06 and P05 respectively. There is also a further shift of the peak sound absorption frequency towards the lower end of the frequency range (Fig. 4). However, the sound absorption of P03 is stronger than that of P06 in general. Fig. 8b shows the spectral variations of τ when P04 is installed. One can notice that this time, while the results at $D = 40$ mm are not changed much, the reduction of sound power transmission relative to that of P06 is only limited to frequencies below 300 Hz. Above that, a general reduction of sound power absorption is observed except for the case of $D = 40$ mm. The τ dip frequencies also shift towards those of the non-perforated panel case of P07.

P03 is more sound absorptive than P06, and one can notice from Fig. 8c that this stronger sound absorption results in very similar or slightly higher τ at frequencies below 500 Hz, but a general reduction of τ otherwise except when $D = 40$ mm where cavity stiffness is relatively strong though P03 is much more sound absorptive than P06. This observation is very similar to that discussed above during the comparison between the results of P05 and P06. Compared to the corresponding results of P04, the reduction of sound transmission is only found at frequencies below ~350–500 Hz in general depending on D, except for the case of $D = 40$ mm where the stronger sound absorption of P03 is expected to appear only after 300 Hz (Fig. 4b). An increase of τ is observed up to nearly 800 Hz in this $D = 40$ mm case. For other cavity depth, the frequency limit of improvement increases with decreasing D.

A different trend is observed when the results of P01, presented in Fig. 8d, are compared with those of P04 (Fig. 8b). The sound absorption of P01 is weaker than that of P04 except at frequencies higher ~730 Hz where P01 is just slightly more sound absorptive than P04. One can notice that the weak sound absorption of P01 here results in nearly broadband increase of τ for all Ds. This is also the case when the results of P01 are compared to those of P03, except for the case of $D = 40$ mm. The case of P02 is much straight-forward, the weak sound absorption of P02 results directly in further increase of τ over the whole frequency range of the present study, though the latter is still lower than that of the non-perforated panel case of P07 (Fig. 5a) because of the sound absorption of P02.

One can notice from Figs. 6 and 8 that the presence of MPP tends to improve broadband sound reduction across the silencer model. However, such effect does not have a straight-forward trend. It is observed

when the MPP has a strong sound absorption capability, its presence tends to strengthen sound transmission across the MPPA silencer model. It is believed that the more dominant panel structural damping is attenuated by the viscous damping produced by the micro-perforations, resulting in the losing sound reduction overall. The cavity stiffness does produce some counteractions, and there is a frequency or a frequency band above which the effect of panel structural damping becomes less dominant in the sound reduction process. In that frequency range, the stronger MPP sound absorption results in higher sound reduction across the silencer model. This observation is highlighted in Fig. 9a with results of P05 and P06 at $D = 160$ mm. P05 is more absorptive than P06 and the frequency of the abovementioned changeover appears to be around 400 Hz. However, there also appears a MPP sound absorption level below which a further reduction gives rise to higher transmitted sound power downstream of the silencer model. An example of this phenomenon is presented in Fig. 9b with results of the weakly absorptive P01 and P02 as examples ($D = 40$ mm).

The increase in panel thickness does not in general result in big changes in the sound power transmission spectra as shown in Fig. 10. For P12 whose sound absorption capacity is comparable to that of P05, the thicker P12 gives rise to higher sound power transmission for $D \leq 80$ mm basically throughout the whole frequency range of the present study as shown in Fig. 10a. The opposite is observed at the other two values of D but at frequencies below ~600 Hz. Above this frequency, P12 gives higher τ. One can observe from Fig. 4 that P12 is less absorptive than P05 at this frequency range when $D = 40$ mm, while when $D = 160$ mm, it is slightly less absorptive than the latter over the whole frequency range of investigation. The higher sound transmission of P05 for $D \geq 120$ mm at frequencies below 600 Hz cannot be the results of the viscous damping at the micro-perforations alone. The cavity stiffness thus has a direct influence in shaping the τ spectra. Also, there is again a frequency or a frequency band which marks a reverse in the trend of the way τ is affected by D (and thus the cavity stiffness).

Increasing s_p reduces the sound absorption capacity of the micro-perforated panel in principle, but can improve the low frequency performance of the panel as shown in Fig. 4c and 4d. At $D = 40$ mm, the weaker sound absorption of P13 results in lower τ as shown in Fig. 10b. The same phenomenon is observed, but the frequency range is reduced with the upper frequency bound shifts lower as D increases. Above that upper frequency bound, τ tends to increase with decreasing panel sound absorption; a phenomenon similar to that observed with the 1.8 mm thick MPPs.

The sound absorption of P10 is in general higher than that of P13, though the low frequency absorption of the latter could get slightly higher as D is reduced. The results shown in Fig. 10c are inline with those observed in Fig. 10a and b. The more sound absorptive P10 gives rise to higher τ below a particular frequency, which tends to decrease with increasing D. At $D = 40$ mm, P10 is less sound absorptive than P13 at frequencies below 400 Hz, and this results in a slightly lower τ than P13 within that frequency range. Basically, the same phenomenon is again observed in Fig. 10d with a further less sound absorptive P11. The corresponding results are thus not discussed.

P08 is the second least sound absorptive MPP in the present study. Similar to P01, the very weak sound absorption leads to higher sound power transmission over the whole frequency range in the present experiment (Fig. 10e). P09 just leads to further broadband increase in τ and thus the corresponding results are not presented. Overall, the observations made with the 2.6 mm thick MPPs are very much inline with those found with the thinner MPPs.

3.3.3. Sound absorption at fixed D

Figs. 6 and 8–10 illustrate that the cavity stiffness, which is reflected by D, plays an important role in the spectral variations of α (and thus τ, as $\tau \approx 1 - \alpha$). In order to understand further such effect, the variations of α of the MPPA silencer models with D are analysed directly. In Fig. 11a–d are presented the spectral variations of α of the 1.8 mm thick MPPs when D, and thus the cavity stiffness, is basically fixed. The difference in the perforation size could have a little effect on the mass density and the overall mechanical strength of the MPP such that the panel stiffness may vary from MPP to MPP. However, it is believed that such change is very small compared to the large change in the cavity stiffness. In Fig. 11, the data below 150 Hz are certainly inaccurate because of the relatively significant sound reflection from the downstream termination of the test rig assembly. They are not discussed.

When $D = 160$ mm, one can observe the same phenomena as illustrated before in Figs. 8 and 9 (Fig. 11a). At low frequencies but higher than 200 Hz, the more absorptive P05 gives the worst α, while α increases as sound absorption capacity of the MPP decreases until the case

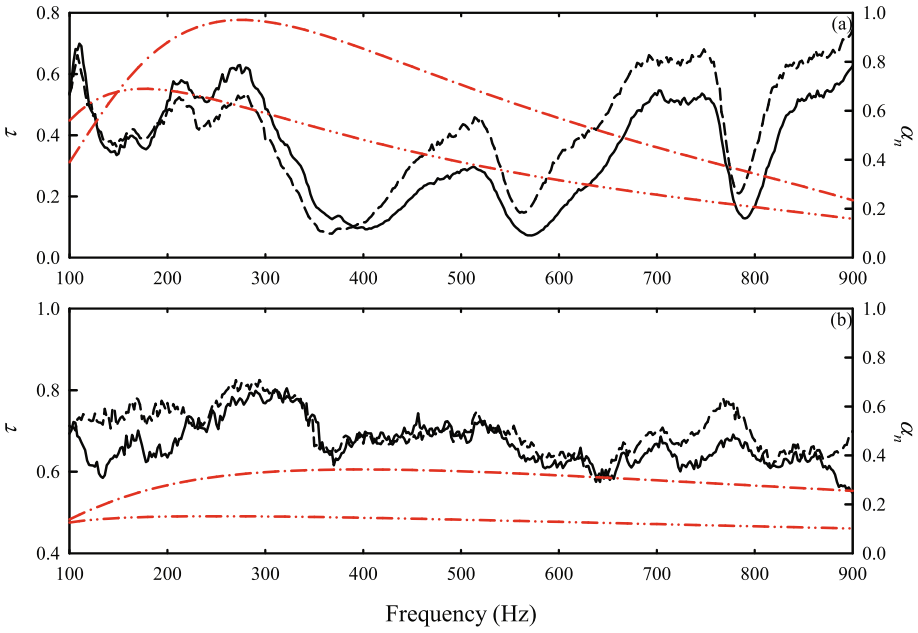

Fig. 9. Examples of τ variation with α_n of MPPs. (a) P05 and P06, $D = 160$ mm. (b) P01 and P02, $D = 40$ mm. ———: τ of P01/P05; – – – –: τ of P02/P06; — · —: α_n of P05/P06; — ·· —: α_n of P01/P02.

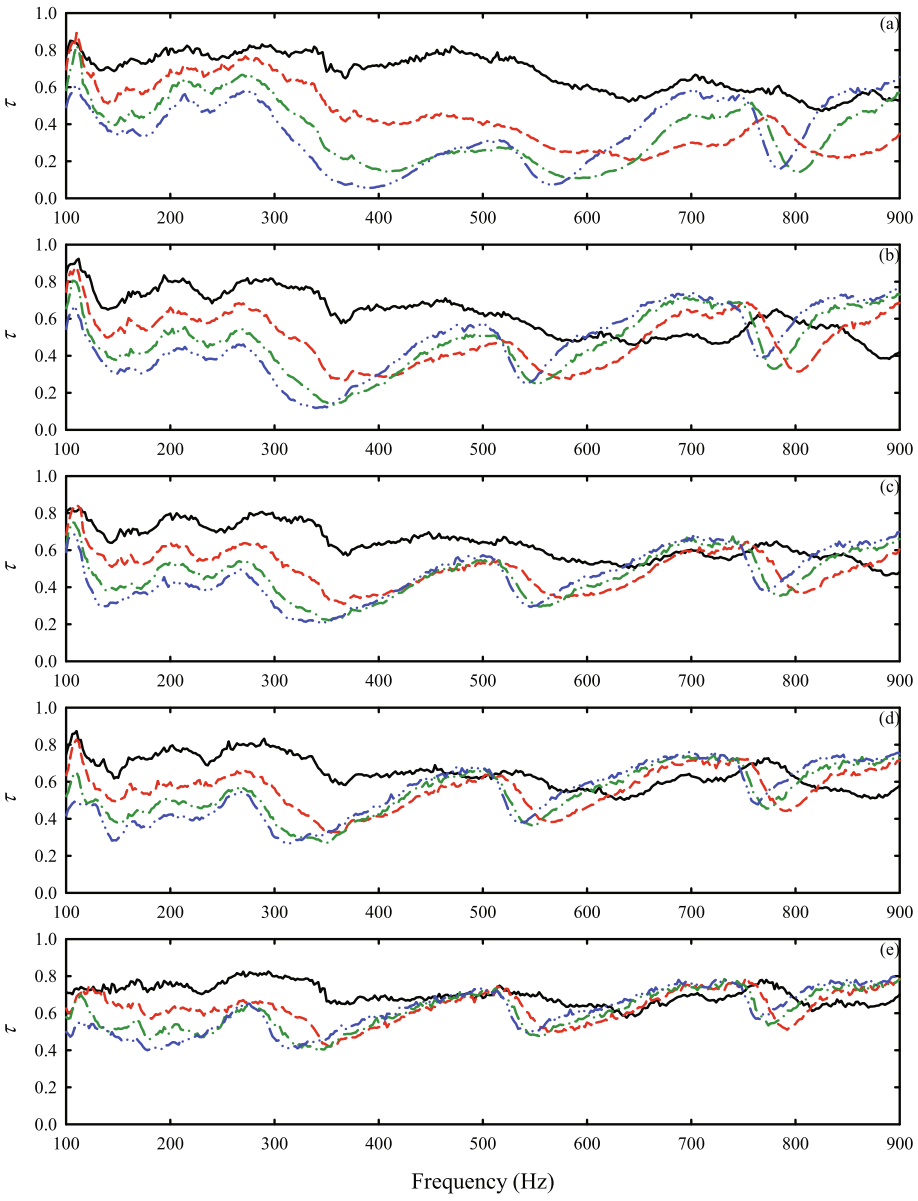

Fig. 10. Effects of MPPs on sound power transmission across the silencer model. t_p = 2.6 mm. (a) P12; (b) P13; (c) P10; (d) P11; (e) P08. Legends: same as those of Fig. 5.

of P04 after which α decreases upon further reduction of MPP sound absorption capacity. This trend changes within a frequency band between 300 Hz and 400 Hz. After that, α increases as the MPP becomes more sound absorptive/dissipative, except within a very narrow band close to the local peak α frequencies. These peaks of α are found near to the frequencies of those obtained with the non-perforated P07 (Fig. 5b), suggesting further the viscous energy damping of the micro-perforations will temper panel vibration and lowering slightly the sound power absorption. There is a little increase in these peak frequencies as the MPP becomes more sound absorptive. For P05/P06/P03, which are more sound absorptive, the α peak at ~300 Hz due to panel vibration should have been masked by their sound absorptions as discussed before with Fig. 7.

The abovementioned trend remains much intact when D is reduced as shown in Fig. 11b and c. There is a shift of the trend changeover band to the higher frequency side of the α spectrum, indicating that the stiffer the cavity relative to the panel, the higher the frequency at which the panel structural damping will become less influential to the overall sound energy transmission. Fig. 11d illustrates the extreme case of a very stiff cavity (D = 40 mm). The changeover cannot even complete at the upper frequency bound of the present study. At this value of D, the variations of α across MPPs is considerably limited compared to those at larger Ds. One can also notice from Fig. 11 that α in general decreases with decreasing D, and so does the sharpness of the α peaks. However, this effect appears to be less serious for less sound absorptive MPPs.

A thicker panel leads to higher flexural modulus and thus its stiffness. Though the panel thickness does not have much impact on the shapes of the α spectra as shown in Fig. 12, it is noticed that the abovementioned changeover of α variation trend takes place and ends at lower frequencies. As the results of the thicker MPPs are very inline with those of the thinner MPPs, Fig. 12 is not further discussed. It is observed that ΔZ does not provide more information regarding the trend and the changeover, and thus it is not presented.

The above-discussed trend of τ (and thus α) variation with MPP sound absorption capacity and the cavity-panel coupling, which appears generic at least within the current parameter range, is relatively complicated. Further investigations are needed to reveal in detail the underlying physics, especially within the frequency range where the

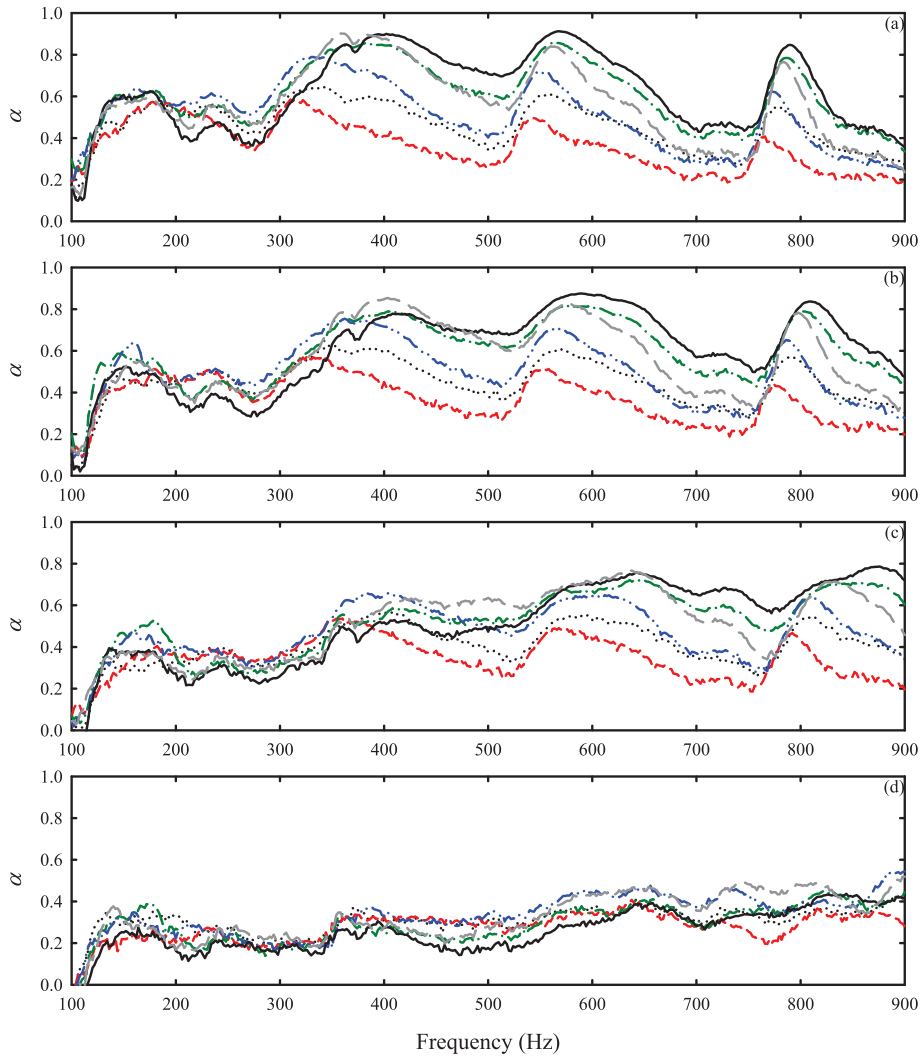

Fig. 11. Effects of cavity depth on the sound power absorption of silencer model with thinner MPPs. $t_p = 1.8$ mm. (a) $D = 160$ mm; (b) $D = 120$ mm; (c) $D = 80$ mm; (d) $D = 40$ mm. · · · · · · · ·: P01; – – – – –: P02; — · —: P03; — ·· —: P04; ———: P05; — —: P06.

changeover occurs.

4. Conclusions

A parametric experimental study was carried out in the present investigation in an attempt to understand the sound transmission across a rectangular duct section installed with a micro-perforated relatively thin duct wall (a four-edge-clamped panel) backed by a rigid sidebranch rectangular chamber (cavity). The effects of the configuration of the micro-perforated duct wall and the depth of the backing cavity on the sound transmission were examined in detail.

A total of 12 micro-perforated panels with different degree of sound absorption and two thicknesses, and the corresponding non-perforated panels were included in the experiments. Owing to limitation of the test rig, the frequency range of the present study is from 200 Hz to 900 Hz, within which only plane waves are significant at the locations of the microphones. Throughout the experiment, the sound power reflection by the test section is weak. Therefore, the sound reduction of the test section mainly comes from the sound absorption of the micro-perforations, the structural energy damping of the vibrating panels and the acoustic impedance within the test section.

Without perforations on the panels, there is evidence that different panel vibration modes are excited by the incident sound wave upon the change of panel thickness. The sound transmission is in general very strong around the eigen-frequencies of the cavity modes, except near the first one where many vibration modes are expected to be excited simultaneously. At higher frequencies, the vibration mode having eigen-frequency just above a cavity mode eigen-frequency will be excited. The excitation of the vibration modes results in some degrees of sound reduction/sound power absorption. As the cavity depth increases, the peak frequencies of sound reduction gradually converge to those of the *in-vacuo* vibration mode eigen-frequencies.

The introduction of micro-perforations gives rise to broadband improvement of sound reduction over the frequency range of the present study in general, though there could be limited deterioration around the lower order vibration mode eigen-frequencies. The present experimental results reveal a complicated trend of sound power transmission variation with the configurations of the micro-perforated panels and the backing cavity depth. For highly sound absorptive panels, a reduction of their sound absorption gives rise to weaker sound power transmission. The stiffness of the backing cavity produces some degrees of tempering to this effect. For larger cavity depth (less stiff cavity), this phenomenon is found below a certain frequency or frequency band, above which the reduction of panel sound absorption results in higher sound transmission. Relatively sharp sound power transmission coefficient dips can also be found at the same time near to the vibration mode eigen-frequencies, suggesting panel vibration damping has become weaker. The very absorptive panels are believed to have attenuated panel

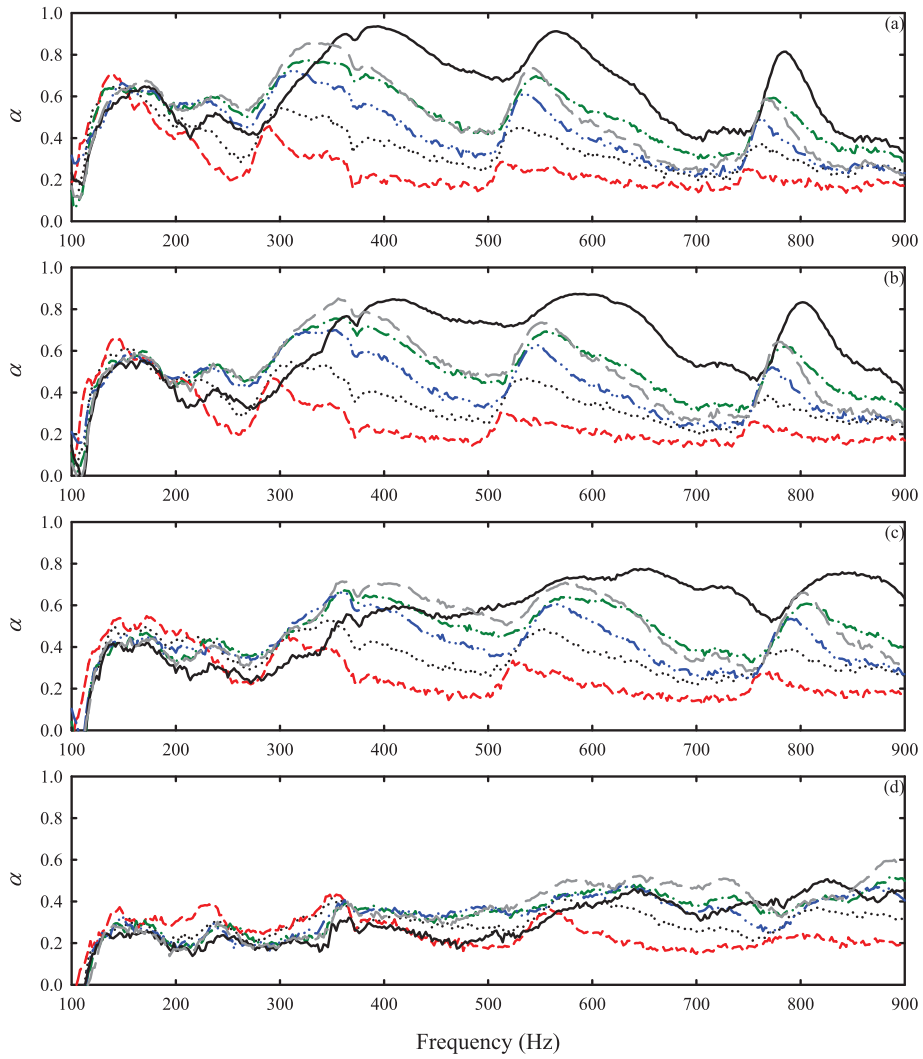

Fig. 12. Effects of cavity depth on the sound power absorption of silencer model with thicker MPPs. $t_p = 2.6$ mm. (a) $D = 160$ mm; (b) $D = 120$ mm; (c) $D = 80$ mm; (d) $D = 40$ mm. · · · · · · · ·: P08; – – – – –: P09; — · —: P10; — ·· —: P11; ———: P12; — —: P13.

vibration, significantly reducing structural energy damping of the panels, before such damping becomes less influential in the sound reduction process at higher frequencies.

For panels of weak sound absorption, sound transmission is instead reduced when stronger absorption is introduced. However, the shapes of sound power transmission spectra remain similar to those obtained with the highly sound absorptive panels. This tends to suggest that there exists a range of MPP absorption in which the contributions of the micro-perforated panel viscous energy dissipation and the panel structural energy damping on the sound transmission process are comparable, and the cavity stiffness becomes crucial in determining the direction of variation on the sound power transmission/absorption spectrum. There is also evidence that an increase of the cavity stiffness relative to that of the MPP panel will tend to shift the frequency range of the above-mentioned changeover of sound power transmission (and thus sound power absorption) variation trend towards the higher frequency side of the spectrum. The exact criteria of the changeover and the related physics are left to further investigations.

CRediT authorship contribution statement

M.L. Fung: Data curation, Formal analysis, Investigation, Methodology, Visualization, Writing – original draft, Writing – review & editing. **S.K. Tang:** Conceptualization, Data curation, Formal analysis, Funding acquisition, Methodology, Project administration, Resources, Supervision, Visualization, Writing – review & editing. **Mors Leung:** Funding acquisition, Resources, Writing – review & editing.

Declaration of competing interest

The authors declare that they have no known competing financial interests or personal relationships that could have appeared to influence the work reported in this paper.

Data availability

Data will be made available on request.

Acknowledgments

The financial supported from the Innovation and Technology Commission, The Hong Kong Special Administration Region Government, China under Project number UIM/360 is gratefully acknowledged. Thanks are also due to Michelle Lung who kindly assisted the conduction of experiments. Her internship was supported by a grant from the Hong Kong Polytechnic University (Grant number: P0014091).

References

[1] Fry A. Noise control in building services. Oxford: Pergamon; 1988.
[2] Beranek LL. Criteria for office quieting based on questionnaire rating studies. J Acoust Soc Am 1956;28(5):833–52.
[3] Harris CM. Handbook of noise control. New York: McGraw-Hill; 1979.
[4] Ingard U. On the theory and design of acoustic resonators. J Acoust Soc Am 1953; 25(6):1037–61.
[5] Tang SK. Narrow sidebranch arrays for low frequency duct noise control. J Acoust Soc Am 2012;132(5):3086–97.
[6] Griffin S, Lane SA, Huybrechts S. Coupled Helmholtz resonators for acoustic attenuation. Trans ASME J Vib Acoust 2001;123(1):11–7.
[7] Seo SH, Kim YH, Kim KJ. Design of silencer using resonator arrays with high sound pressure and grazing flow. Appl Acoust 2018;138:188–98.
[8] Howard CQ, Cazzolato BS, Hansen CH. Exhaust stack silencer design using finite element analysis. Noise Control Eng J 2000;48(4):113–20.
[9] Gao N, Zhang Z, Deng J, Guo X, Cheng B, Hou H. Acoustic metamaterials for noise reduction: A review. Sci Rep 2017;7(1):2100698.
[10] Maa D-Y. Potential of microperforated panel absorber. J Acoust Soc Am 1998;104 (5):2861–6.
[11] Liu J, Hua X, Herrin DW. Estimation of effective parameters for micro-perforated panel absorbers and application. Appl Acoust 2014;75:86–93.
[12] Sakagami K, Nakamori T, Morimoto M, Yairi M. Double-leaf microperforated panel space absorbers: A revised theory and analysis. Appl Acoust 2009;70(5):703–9.
[13] Bravo T, Maury C, Pinhède C. Sound absorption and transmission through flexible micro-perforated panels backed by an air layer and a thin plate. J Acoust Soc Am 2012;131(5):3853–63.
[14] Fung ML, Tang SK, Leung M. Modelling the sound absorption of panels with tapered elliptic micro-perforations. Appl Acoust 2023;213:109654.
[15] Allam S, Åbom M. A new type of muffler based on microperforated tubes. ASME Trans J Vib Acoust 2011;133(3):031005.
[16] Takahashi D, Tanaka M. Flexural vibration of perforated plates and porous elastic materials under acoustic loading. J Acoust Soc Am 2002;112(4):1456–64.
[17] Wang C, Cheng L, Pan J, Yu G. Sound absorption of a micro-perforated panel backed by irregular-shaped cavity. J Acoust Soc Am 2010;127(1):238–46.
[18] Yu HM, Tang SK. Sound transmission across a narrow sidebranch array duct muffler at low Mach number. J Acoust Soc Am 2020;148(3):1692–702.
[19] Tang SK, Tang YJ. On the length scale and Strouhal numbers for the sound transmission across coupled duct cavities at low Mach number. J Acoust Soc Am 2021;150(6):4232–43.
[20] Neise W, Frommhold W, Mechel FP, Holste F. Sound power determination in rectangular flow ducts. J Sound Vib 1994;174(2):201–37.
[21] Tang SK, Li FYC. On low frequency sound transmission loss of double side-branches: a comparison between theory and experiment. J Acoust Soc Am 2003; 113(6):3215–25.
[22] Chung JY, Blaser DA. Transfer function method of measuring in-duct acoustic properties. I. Theory. J Acoust Soc Am 1980;68(3):907–13.
[23] Cremer L. Theory regarding the attenuation of sound transmitted by air in a rectangular duct with an absorbing wall, and the maximum attenuation constant produce during the process. Acust 1953;3:249–63 [in German].
[24] Lee YY, Lee EWM, Ng CF. Sound absorption of a finite flexible micro-perforated panel backed by an air cavity. J Sound Vib 2005;287(1–2):227–43.
[25] Bravo T, Maury C, Pinhède C. Vibroacoustic properties of thin micro-perforated panel absorbers. J Acoust Soc Am 2012;132(2):789–98.
[26] Pretlove AJ. Free vibrations of a rectangular panel backed by a closed rectangular cavity. J Sound Vib 1965;2(3):197–209.
[27] Leissa AW. Vibration of plates. New York: A.I.P; 1993.
[28] Tang SK. Sound transmission characteristics of Tee-junctions and the associated length corrections. J Acoust Soc Am 2004;115(1):218–27.
[29] Zhang X, Cheng L. Broadband and low frequency sound absorption by sonic black holes with micro-perforated boundaries. J Sound Vib 2021;512:116401.
[30] Bravo T, Maury C. Broadband sound attenuation and absorption by duct silencers based on the acoustic black hole effect: simulations and experiments. J Sound Vib 2023;561:117825.
[31] Munjal ML. Acoustics of ducts and mufflers. New York: Wiley; 1987.